Construction and the ergodicity properties of dual unitary quantum circuits

Márton Borsi and Balázs Pozsgay ⓘ

MTA-ELTE "Momentum" Integrable Quantum Dynamics Research Group, Department of Theoretical Physics,
Eötvös Loránd University, Pázmány Péter stny. 1A, Budapest 1117, Hungary

We consider one-dimensional quantum circuits of the brickwork type, where the fundamental quantum gate is dual unitary. Such models are solvable: the dynamical correlation functions of the infinite temperature ensemble can be computed exactly. We review various existing constructions for dual unitary gates and we supplement them with new ideas in a number of cases. We discuss connections with various topics in physics and mathematics, including quantum information theory, tensor networks for the AdS/CFT correspondence (holographic error correcting codes), classical combinatorial designs (orthogonal Latin squares), planar algebras, and Yang-Baxter maps. Afterwards we consider the ergodicity properties of a special class of dual unitary models, where the local gate is a permutation matrix. We find an unexpected phenomenon: nonergodic behavior can manifest itself in multisite correlations, even in those cases when the one-site correlation functions are fully chaotic (completely thermalizing). We also discuss the circuits built out of perfect tensors. They appear locally as the most chaotic and most scrambling circuits, nevertheless they can show global signs of nonergodicity: if the perfect tensor is constructed from a linear map over finite fields, then the resulting circuit can show exact quantum revivals at unexpectedly short times. A brief mathematical treatment of the recurrence time in such models is presented in Appendix (written by Roland Bacher and Denis Serre).

I. INTRODUCTION

Interacting many body systems are typically not amenable to analytic solution, neither in classical nor in quantum mechanics, and their exact treatment is possible only in a very limited set of models. Somewhat trivial examples are models which are equivalent to free bosons of free fermions: in these cases the dynamics is one-body reducible and all correlation functions can be computed using Wick's theorem. If there are interactions in the system, then one needs to impose some sort of restrictions on the dynamics such that it remains tractable.

One class of such systems are the so-called one-dimensional integrable models. In this case solvability is guaranteed by the existence of a large (typically infinite) family of local conserved charges, leading to completely elastic and factorized scattering of the quasiparticles [1]. This implies the lack of ergodicity, and as a result isolated integrable models equilibrate to Generalized Gibbs Ensembles (see the review [2]).

Dual unitary (DU) quantum circuits are an other class of exactly solvable systems [3–5]. In these models, the solvability follows from a special property of the basic two-site quantum gate: dual unitarity means that the fundamental quantum gate is unitary also when viewed as a generator of dynamics in the space direction. The dual unitarity condition is equivalent to having a two-site unitary gate with maximal bipartite operator entanglement [6]. The distinguishing physical behavior of DU circuits is that the dynamical two-point correlation functions (computed in the infinite temperature ensemble) are nonzero only along light cones [5]. DU circuits

can be chaotic or integrable (precise definitions will be given in the main text); it is remarkable that even the chaotic DU circuits are solvable.

DU circuits received considerable attention in the recent years, and their correlation functions and entangling properties were studied in depth, see, for example, Refs. [6–14]. Their computational power from an information theoretical perspective was considered in Ref. [15]. A full classification of DU gates is available for local dimension $N = 2$ [5], but some constructions are known in the literature also for $N \geqslant 3$ which will be reviewed in Sec. III. A numerical method for the production of DU gates was presented in Ref. [16].

A special class of DU gates are those which have maximal entangling power: these are perfect tensors [17–19]. In quantum information theory, a perfect tensor is a vector of a multisite Hilbert space, which has maximal bipartite entanglement for all possible partitioning of its sites (also called parties or tensor legs). Alternatively, for an even number of legs they can be seen as multiunitary operators for every bipartitioning of the legs into two subsets with equal size [20]. Such states are also called absolutely maximally entangled (AME) states, and they have been studied in a large number of works, see, for example, Refs. [18,20–22] and references therein. A list of AME states with various numbers of legs and local dimensions is available at the homepage [23]. Dual unitary gates which are also perfect tensors correspond to AME states with four legs. It is known that such states exist for all local dimensions except for $N = 2$ [24]; the last remaining open case of $N = 6$ was solved very recently [25]. Perfect tensors can be used as quantum error correcting codes, and

they are essential ingredients in the tensor network models of the AdS/CFT bulk-boundary correspondence (see the seminal paper [26] and the recent review [27]).

Dual unitary gates can be seen as "broken" or "imperfect" versions of the perfect tensors with four legs. Research on quantum error correcting codes and especially on holographic codes led to the introduction of such "broken" or weaker versions of "perfectness." The work [28] introduced perfect tangles, which are multileg tensors that have maximal entanglement for all "planar" bipartitions; the dual unitary gates correspond to perfect tangles with four legs. The same definition was given independently in Ref. [29] and in Ref. [30], where the same objects were called "block perfect tensors" and "planar maximally entangled states," respectively. The tri-unitary quantum gates considered recently in Ref. [31] are six-leg tensors which are perfect tangles.

Time evolution in a quantum circuit with a perfect tensor was studied already in 2015 in Ref. [19]. It was shown here that the resulting circuit generates ballistic growth of operator entanglement, and it is a good toy model for scrambling of quantum information. More recently circuits built from so-called perfect DU gates were also studied in Ref. [6], where they were called "Bernoulli circuits" (for a definition see the main text). These circuits can be seen as the most chaotic ones, at least from a local perspective: all dynamical correlation functions vanish in the infinite temperature ensemble. In the tensor network models of AdS/CFT the analogous behavior was observed in Ref. [32]. Nevertheless, such circuits can also show global signs of integrability [19]; we discuss this phenomenon in Sec. V.

Dual unitary matrices have a connection with pure mathematics, which has not yet been noticed in the relevant condensed matter literature: they appear in the study of planar algebras. This theory originates from the work of Vaughan Jones [33], building on earlier works on von Neumann algebras (see the book [34] of Jones and Sunder). The notion of dual unitarity (called biunitarity in the mathematical literature) appears in this theory. Implications for quantum information theory were studied in Ref. [35] and more recently in Ref. [36]. The general concept of biunitarity treated in these works accommodates not only the actual DU gates, but also complex Hadamard matrices, quantum error correcting codes, and quantum Latin squares. The very special case of dual unitary permutation matrices was studied already in 1996 in Ref. [37], where a complete enumeration was given for local dimensions $N = 2$ and 3.

In this work, we set ourselves two goals.

(1) We collect a number of constructions for DU gates that appeared in various places in the literature, and we complement them with new ideas. After a technical introduction in Sec. II the constructions are discussed in Sec. III.

(2) We treat the ergodicity properties of DU circuits with permutation maps. These circuits can be understood as classical cellular automata, but it is useful to treat them also as quantum objects. We uncover interesting physical phenomena in these models. We show that there are models which appear fully chaotic on the level of one-site correlations, but which display nonergodicity if we look at the multisite reduced density matrices. The possible existence of such behavior was already mentioned in Ref. [5] (see also the so-called
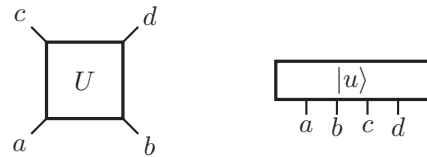

FIG. 1. Pictorial representation of a DU gate. On the left, the gate is pictured as a four leg tensor, which can generate unitary dynamics in both the time and space directions. For forward time evolution, the incoming indices are a and b, whereas for "forward space evolution" they are c and a. On the right, the same object is pictured as a vector of a fourfold product space. If the gate is DU, then the vector $|u\rangle$ is maximally entangled with respect to subsystems given by the pairs (a, b), (a, c) and their complements. It is a perfect tensor if maximal entanglement also holds for the subsystem given by the pair (a, d).

"still gliders" found in Ref. [38]) and now we find concrete examples for this; this discussion is presented in Sec. IV. Afterwards we also investigate global signs of nonergodicity in DU circuits built from perfect maps. These findings are presented in Sec. V, complementing the relevant results of the earlier work [19]. A mathematical treatment of the recurrence time in a special class of models (given by linear maps over finite fields) is given in Appendix.

II. DUAL UNITARY CIRCUITS

We consider a spin chain with a Hilbert space $\mathcal{H} = \otimes_{j=1}^{L} \mathbb{C}^N$, where the local dimension N is a fixed number of the system, and L is the volume which we assume to be an even number. We build a quantum cellular automaton on this Hilbert space, such that the time evolution is dictated by a quantum circuit of the brickwork type. The fundamental object is a two site unitary gate U, which is a linear operator on $\mathbb{C}^N \otimes \mathbb{C}^N$. If $|\Psi(t)\rangle \in \mathcal{H}$ is the state of the system at time t, then the update rule of the QCA is such that

$$|\Psi(t+1)\rangle = \begin{cases} \mathcal{V}_1|\Psi(t)\rangle & \text{for } t = 2k+1, \\ \mathcal{V}_2|\Psi(t)\rangle & \text{for } t = 2k \end{cases}, \quad (1)$$

where the alternating update operations are

$$\mathcal{V}_1 = U_{12}U_{34} \ldots U_{L-1,L}, \quad (2)$$

$$\mathcal{V}_2 = U_{23}U_{45} \ldots U_{L,1}. \quad (3)$$

Here periodic boundary conditions are assumed. For further use we also introduce the Floquet operator

$$\mathcal{V} = \mathcal{V}_2 \mathcal{V}_1, \quad (4)$$

which generates time evolution from time t to $t + 2$.

We are interested in the special case when U is a dual-unitary operator [3–5]. The dual unitary condition is formulated as follows.

Let us choose a basis in $\mathbb{C}^N$ and denote U_{ab}^{cd} the matrix elements of the operator U in the given basis. We use the reshuffled matrix U^R given by

$$(U^R)_{ca}^{db} = U_{ab}^{cd} \quad (5)$$

and say that U is dual unitary if it is unitary and also U^R is unitary. For a pictorial representation see Fig. 1.

Using the SWAP gate $\mathcal{P}$ given by

$$\mathcal{P}^{cd}_{ab} = \delta_{ad}\delta_{bc}, \qquad (6)$$

we can see that $\mathcal{P}U^R = U^{t_2}$, where the superscript t_2 stands for partial transpose in the second component. The swap gate is unitary, thus a bipartite unitary matrix U is dual unitary, iff its partial transposes are unitary. The latter property was called "biunitary" in the earlier mathematical literature dealing with von Neumann algebras [34,37]. The simplest dual unitary gate is the SWAP gate itself.

The dual unitarity condition implies a certain space-time duality: if we picture the resulting time evolution as a tensor network, then this network describes unitary evolution also in the space direction. This property has important consequences which we discuss below in Sec. II A.

A special class of DU matrices are the so-called perfect tensors (or 2-unitaries) [20]. In order to introduce them, we define one more reshuffling as

$$(U^D)^{bc}_{ad} = U^{cd}_{ab}. \qquad (7)$$

It can be seen that U^D acts "from diagonal to diagonal", see also Fig. 1. A DU gate is a perfect tensor if U^D is also unitary matrix. In this work we refer to such matrices as perfect DU gates. The algebraic variety of such matrices was studied in Ref. [39]. The resulting quantum circuits were analyzed in Ref. [6], where they were called Bernoulli gates. It is known that perfect tensors exist for all integers $N \geqslant 3$: the long standing open problem of the case $N = 6$ was solved very recently [25].

For qubits DU gates, were completely classified in Ref. [5], but there is no general parametrization of DU gates known for $N \geqslant 3$. Instead, several concrete constructions appeared in the literature. We discuss these constructions later in Sec. III.

A. Correlation functions and conserved charges

Physical properties of dual unitary circuits were studied in depth in the literature [6–12,14]. One of the central results is that one-site correlation functions are nonzero only along light cones. To be more precise, let us consider two one-site operators $o_1(x)$ and $o_2(y)$ and the infinite temperature average of the dynamical correlation function

$$\langle o_1(x,t)o_2(y,0)\rangle \equiv \frac{1}{N^L}\mathrm{Tr}(o_1(x,t)o_2(y,0)), \qquad (8)$$

where it is understood that time evolution of the operator is dictated by the adjoin action of the Floquet operator $\mathcal{V}$. The central result of Ref. [5] is that such two-point functions can be nonzero only if $|x - y| = t$. Furthermore, their precise values are determined by the eigenvalues of two quantum channels (light cone propagators for the operators). To be precise, let us define the linear maps $M_\pm$ acting on one-site operators as

$$M_+(o) = \frac{1}{N}\mathrm{Tr}_1(U^\dagger(o\otimes 1)U), \quad M_-(o) = \frac{1}{N}\mathrm{Tr}_2(U^\dagger(1\otimes o)U). \qquad (9)$$

Eigenvalues of these maps determine the behavior of the correlation functions along the right moving and left moving light cones, respectively. An eigenvalue $\lambda = 1$ corresponds

to a conserved one site operator, which we also call glider (see below). Note that the identity operator $o = 1$ always has $\lambda = 1$ by unitarity. Eigenvalues $|\lambda| = 1$ different from 1 describe oscillating behavior, and eigenvalues $|\lambda| < 1$ correspond to thermalizing modes. If all nontrivial eigenvalues are thermalizing, then the circuit was interpreted as ergodic and mixing [5].

A dual unitary model can also have multisite conserved charges. In order to discuss them, we introduce the concept of gliders. Following Ref. [40], we say that a short range operator $\mathcal{O}(x)$ positioned at site x is a glider if its time evolution gives

$$\mathcal{O}(x, t + 1) = \mathcal{O}(x \pm 1, t), \qquad (10)$$

where the signs $+$ and $-$ stand for right moving and left moving gliders, respectively. In the formula above time evolution is understood in the Heisenberg picture, dictated by the e.o.m. (1). The equation above means that gliders do not suffer operator spreading, and summation over x gives an extensive conserved charge of the model. It was shown in Ref. [9] that in a DU circuit all conserved charges come from gliders.

It is useful to extend the definition of the gliders to allow for periodic oscillations, so that

$$\mathcal{O}(x, t + 1) = e^{i\phi}\mathcal{O}(x \pm 1, t), \qquad (11)$$

where $e^{i2n\phi} = 1$ with some n. In such cases, the operator appears exactly conserved if we sample the system stroboscopically with period $2n$.

The relation (11) can be written more explicitly as the exchange relation

$$\mathcal{O}(x)\mathcal{U}^{-2}\mathcal{V} = e^{2i\phi}\mathcal{U}^{-2}\mathcal{V}\mathcal{O}(x), \qquad (12)$$

where $\mathcal{U}$ is the cyclic shift operator on the lattice and $\mathcal{V}$ is the Floquet operator defined in (4). For left moving gliders, we have an analogous relation with $\mathcal{U}^{-2}$ exchanged by $\mathcal{U}^2$.

The fact that all conserved charges are gliders makes the search for them especially simple: One has to look for solutions of the linear equation (12) within the vector space of local operators, with some eigenvalues λ that are roots of unity.

Equation (12) implies that gliders form an operator algebra which is closed under addition and multiplication. Therefore, if a DU circuit has at least one conserved charge, then it has infinitely many: equal-time products of gliders moving in the same direction are also gliders [8,9].

As an alternative to solving (12), we can also consider the multisite transfer matrices that propagate extended local operators along light cone directions [5] and look again for the number of eigenvalues that are roots of unity. These transfer matrices were first introduced in Refs. [38,41] and they are constructed as follows.

For a DU gate U, we introduce two more two-site gates as

$$V = \mathcal{P}U^\dagger, \quad V' = \mathcal{P}U^R. \qquad (13)$$

The action of the linear map in M_+ from (9) can be rewritten as the action of a transfer matrix on the doubled Hilbert space $\mathbb{C}^N \otimes \mathbb{C}^N$. Let A stand for an auxiliary space and define the matrix product operator

$$t = \frac{1}{N}\mathrm{Tr}_A[V'_{2,A}V_{1,A}]. \qquad (14)$$

In this case, the eigenvectors of t correspond to the eigenoperators of M_+. The extension to multisite channels is a transfer matrix acting on an auxiliary chain of length 2α such that

$$t_\alpha = \frac{1}{N}\text{Tr}_A\left[V'_{2\alpha,A}\ldots V'_{\alpha+1,A}V_{\alpha,A}\ldots V_{2,A}V_{1,A}\right]. \quad (15)$$

This transfer matrix also appeared in Ref. [41], see Eq. (7) there. It describes the evolution of multisite operators along the positive light directions, for a maximal range of $2\alpha - 1$ (for a more detailed derivation see Ref. [41]). The number of right moving gliders of maximal range $2\alpha - 1$ can be found simply by counting the eigenvalues λ of the operator $t_\alpha = 1$ which are roots of unity. For the left moving gliders, one just performs a space reflection of the original gate U.

In DU circuits with perfect tensors, a very special phenomenon happens: it was shown in Ref. [6] that in such cases, all nontrivial nonequal-time correlations are zero in the infinite temperature ensemble. This means that the spectra of the t_α (and their space reflected variants) are trivial: they have a single trivial eigenvalue $\lambda = 1$ and all remaining eigenvalues are zero. This forbids the existence of local conserved charges in such models. Perfect tensors should be interpreted as "most ergodic" in the hierarchy of DU circuits. The vanishing of the connected correlation functions in tensor network models with perfect tensors was also observed in Ref. [32]. The property of "maximal ergodicity" underlies the application of perfect tensors in lattice models of the AdS/CFT correspondence [26,27].

B. Entanglement of operators and states

It is useful to discuss the entanglement properties of dual unitary gates. The standard method is to picture the operator as a vector of a doubled Hilbert space (see Fig. 1).

To every unitary operator U acting on a bipartite system we can associate a four partite state $|u\rangle \in \mathcal{H}_1 \otimes \mathcal{H}_2 \otimes \mathcal{H}_3 \otimes \mathcal{H}_4$, where each $\mathcal{H}_j \simeq \mathbb{C}^N$ and in a concrete basis the components are $u_{abcd} = U_{ab}^{cd}/N$. The factor $1/N$ is added so that $|u\rangle$ is normalized to unity. Entanglement properties of the gate U can be understood as different sorts of entanglement of the state $|u\rangle$.

Let us consider reduced density matrices of the states $|u\rangle$ corresponding to pairs of sites. To this order, we introduce the set $S = \{1, 2, 3, 4\}$ of "sites" or "parties" and define the reduced density matrices

$$\rho_{\alpha\beta} = \text{Tr}_{S\setminus\{\alpha,\beta\}}|u\rangle\langle u|, \quad \alpha, \beta \in S. \quad (16)$$

The unitarity of the gate U implies that ρ_{12} and ρ_{34} are proportional to the identity matrix. This means that $|u\rangle$ has maximal entanglement between subsystems (1,2) and (3,4). Similarly, dual unitarity means that ρ_{13} and ρ_{24} are also proportional to the identity, which means maximal entanglement between subsystems (1,3) and (2,4). This also means that as an operator U has maximal operator entanglement between the two sites on which it acts.

Then the only remaining bipartite entanglement measure is the "diagonal entanglement" of the gate, which is the entanglement between subsystems (1,4) and (2,3), to be computed from ρ_{14} or ρ_{23}. If this entanglement is also maximal, then the state $|u\rangle$ is said to be absolutely maximally entangled, or

equivalently, a perfect tensor. It can be shown that for dual unitary gates the so-called "entangling power" of the gate [42] depends only on the "diagonal entanglement" [6], and it is maximal for perfect tensors.

We say that a DU gate is noninteracting if the diagonal entanglement is zero. It can be shown that in these cases

$$U = (A \otimes B)\mathcal{P} \quad (17)$$

with some $A, B \in U(N)$. The resulting time evolution of the quantum circuit is trivial: there is no interaction between qudits propagating on the different light cones.

III. CONSTRUCTIONS FOR DU GATES

In this section, we discuss a number of different constructions for DU gates. Most of them already appeared in the literature, but we also include new ideas; in each case it will become clear from the text whether it is a known construction or a new addition. In most of the examples, we treat homogeneous cases, when the two sites on which the dual unitary acts have the same dimension. However, sometimes we also consider nonhomogeneous cases.

Before turning to the constructions let us discuss equivalence classes of DU gates. First of all, unitarity, dual unitarity and also the perfect tensor property are preserved by dressing with one-site unitaries. This means that if U satisfies these properties, then for any $A, B, C, D \in U(N)$ the matrix

$$\tilde{U} = (A \otimes B)U(C \otimes D) \quad (18)$$

also satisfies them.

For every DU gate U, the reshuffled gate U^R is also dual unitary, this follows from the construction. Furthermore, for each U we can define the space-reflected and time reflected gates as

$$\mathcal{P}U\mathcal{P}, \quad \mathcal{T}U\mathcal{T} = U^t = U^{t_1 t_2}, \quad (19)$$

Both the space and the time reflections preserve dual unitarity. Note that we did not include a complex conjugation in the definition of the time reflection; this has no physical meaning at this point, it is a mere convenience for the classification. The three discrete transformations generate the group D_4, which is the geometric symmetry group of the square: the transformations can be seen as permutations of the legs of the tensor U such that the diagonals are preserved. In contrast, for perfect tensors, an arbitrary permutation of the four legs is an allowed transformation.

The transformations can be used to define equivalence classes of DU gates. However, different members of each class can lead to quantum circuits with very different physical behavior: for example fine tuned integrable gates can be made completely ergodic by multiplication with one-site unitaries.

For the discussion of the various constructions, it is useful to focus only on the equivalence classes. Therefore, in the sections below, we will not discuss the addition of the one-site unitaries.

Later in Sec. IV, we also need equivalence classes of quantum circuits, such that two circuits in the same class are equivalent to each other. Diagonal dressings of the type

$$\tilde{U} = (A \otimes B)U(B^\dagger \otimes A^\dagger), \quad A, B \in U(N) \quad (20)$$

lead to equivalent circuits, because the one-site unitaries cancel on the diagonal links in the circuit. This diagonal dressing will be used an equivalence relation in Sec. IV.

In some of the constructions below, we will use nonhomogeneous gates, that act on two spaces with different local dimensions. In such cases, it is always understood that the gate permutes the order of the spaces in the tensor product. For example, let us choose two natural numbers N and M and consider the linear operator U acting on $\mathbb{C}^N \otimes \mathbb{C}^M \to \mathbb{C}^M \otimes \mathbb{C}^N$. In such a case, we say that the gate is of type (N, M). The DU condition is naturally extended to these nonhomogeneous cases.

A. Complete classification for $N = 2$

For qubits, the complete characterization of DU gates was performed in Ref. [5]. It was found that each DU gate is equivalent to the matrix

$$U = \begin{pmatrix} e^{-iJ} & & & \\ & & -ie^{iJ} & \\ & -ie^{iJ} & & \\ & & & e^{-iJ} \end{pmatrix}, \quad J \in \mathbb{R}. \quad (21)$$

This matrix can be seen as a dressing of the SWAP gate with some phases. Conventions are chosen such that they coincide with the formulas of Ref. [5].

These gates are never perfect tensors, in accordance with the fact that there is no perfect tensor with four legs for $N = 2$ (see, for example, Ref. [24]).

B. Dressed SWAP gates for $N \geqslant 3$

In Ref. [43], the following construction was published for all N:

$$U = D\mathcal{P}, \quad (22)$$

where $\mathcal{P}$ is the SWAP gate and D is a diagonal unitary matrix of size $N^2 \times N^2$. Dual unitarity is easily established, because the reshuffling leads to a gate of precisely this form, with the elements of D reshuffled.

These gates are never perfect tensors, but they have nonzero entangling power: the phases included in the matrix D create entanglement between qudits propagating on the different light cones [6,43].

C. Direct sums

Various types of block diagonal constructions (or direct sums) appeared in Refs. [6,16,44]. The basic idea is to consider subspaces which are kept invariant in the diagonal direction.

Let us consider gates of type (N, M) and let us split N into a sum of two-nonzero integers N_1, N_2. Let U_1 and U_2 be dual unitary gates of types (N_1, M) and (N_2, M). Then a DU gate of type (N, M) is obtained as

$$U = U_1 \oplus U_2. \quad (23)$$

Here it is understood that the product spaces are split as

$$\mathbb{C}^N \otimes \mathbb{C}^M = (\mathbb{C}^{N_1} \otimes \mathbb{C}^M) \oplus (\mathbb{C}^{N_2} \otimes \mathbb{C}^M),$$
$$\mathbb{C}^M \otimes \mathbb{C}^N = (\mathbb{C}^M \otimes \mathbb{C}^{N_1}) \oplus (\mathbb{C}^M \otimes \mathbb{C}^{N_2}), \quad (24)$$
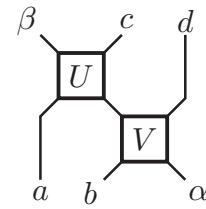

FIG. 2. Diagonal composition of two nonhomogeneous DU gates.

and U_j with $j = 1, 2$ act as $\mathbb{C}^{N_j} \otimes \mathbb{C}^M \to \mathbb{C}^M \otimes \mathbb{C}^{N_j}$. As an effect of the diagonal arrangement of the splitting the invariant subspaces are also conserved for the reshuffled matrices, and dual unitarity of U follows immediately.

The splitting of the subspaces can be performed on both spaces, and it can be repeated any desired number of times.

As an extreme case of this construction we obtain controlled unitaries. Let us consider a gate of type (N, N) and let us split the first space into a direct sum of N one-dimensional spaces. Then the above construction gives

$$U = \mathcal{P}\left[\sum_{j=1}^{N} P_1^j U_2^{(j)}\right], \quad (25)$$

where $\mathcal{P}$ is the SWAP gate, $P^j = |j\rangle\langle j|$ are projectors to local basis states, and $U^{(j)}$ are N unitaries of size $N \times N$.

D. Diagonal compositions

The product of two DU gates is not dual unitary, but a certain diagonal composition preserves dual unitarity [35].

Let us choose three natural numbers N_1, N_2 and M, and consider two dual unitary gates U and V, which are of type (N_1, M) and (N_2, M), respectively. Then we can construct a new gate Z of type $(N_1 N_2, M)$ as

$$Z_{ab,\alpha}^{\beta,cd} = U_{a\gamma}^{\beta c} V_{b\alpha}^{\gamma d}, \quad (26)$$

where the basis states of the product space $\mathbb{C}^{N_1} \otimes \mathbb{C}^{N_2}$ are indexed with pairs of indices a, b and c, d, and the Greek indices stand for the basis states in $\mathbb{C}^M$. The dual unitarity of Z follows from the fact that it is a product of unitary gates in both the time and space directions. For a pictorial interpretation see Fig. 2.

As usually, the DU gate in Eq. (26) can be dressed by one site unitaries, which act on the local spaces of dimension $N_1 N_2$ and M. This allows for more freedom than just the dressing of the gates U and V separately.

The steps of construction can be repeated, and various composites can be formed. For example a large family of (homogeneous) DU gates for $N = 4$ can be constructed using the decomposition $\mathbb{C}^4 = \mathbb{C}^2 \otimes \mathbb{C}^2$. In the following we write down an explicit formula for $N = 4$.

We use the following notations: we regard the two-site space $\mathbb{C}^4 \otimes \mathbb{C}^4$ as the four-site product $\otimes_1^4 \mathbb{C}^2$, we work with operators acting on pairs of qubits, and when writing down the formula we omit the indices of the matrices and just denote the indices of the spaces on which the two-qubit operators act. Let C be an arbitrary two-site unitary, and X, Y, V, Z be DU gates, all corresponding to $N = 2$. Then a DU gate for $N = 4$
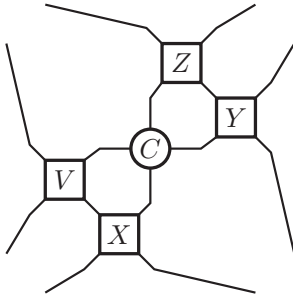
FIG. 3. Diagonal composition of qubit gates, in order to obtain a DU gate for $N = 4$ [representation of formula (27)]. The rectangles stand for DU gates, and the circle denotes an unitary operator C (not necessarily DU). The resulting circuit is dual unitary, because it is a product of unitary operators in both the time and space directions.

is constructed as

$$U = Z_{23}Y_{34}C_{23}V_{12}X_{23}. \tag{27}$$

This operator is clearly unitary, because it is a product of unitary operators. The dual unitarity can be established step by step, noting that the reshuffled operator (which acts in the space direction) is also a product of unitary operators with a well defined order of their action. For a graphical interpretation of this operator see Fig. 3. The dual unitarity is easily read off this figure.

For $N = 2$, the most general unitary and dual unitary matrices are known explicitly (for the DU case see Sec. III A above), therefore Eq. (27) gives an explicit parametrization of a large class of DU gates for $N = 4$.

These diagonal compositions can be seen as special cases of the constructions treated in the papers [35,36], which deal with a more general notion of biunitarity. The specific formulas we gave appear to be new.

E. Permutation circuits: generalities

A permutation matrix is a unitary operator U whose matrix representation is deterministic in a chosen basis. This means that for any pair of local basis states $|a\rangle \otimes |b\rangle$, we have

$$U(|a\rangle \otimes |b\rangle) = |c\rangle \otimes |d\rangle, \tag{28}$$

where $c = c(a, b)$ and $d = d(a, b)$. With some loose notation we will also write $U(a, b) = (c, d)$, in which case U is understood as a map $X^2 \to X^2$ where $X = \{1, \dots, N\}$. Unitarity implies that U is invertible as a map: it describes a bijection between pairs of variables (a, b) and (c, d).

A quantum circuit constructed from a permutation matrix could be understood as a classical cellular automaton, but it is useful to regard them as special cases of a QCA. Even though such gates are deterministic, generally they create quantum entanglement in the system [45].

The permutation map U is dual unitary, if it also describes a bijection between the pairs of variables (a, c) and (b, d). Lacking a better name, such gates can be be called dual unitary permutation matrices. With regards to quantum circuits they have been studied recently in Ref. [6], but they appeared much earlier in the mathematical literature. The first work

TABLE I. Two representations of a dual unitary permutation matrix with $N = 3$. On the left: representation as a broken orthogonal array. On the right: representation as a pair of orthogonal squares, C being row-Latin and D being column-Latin. As a pair, they are denoted together as CD.

a	b	c	d		
1	1	3	3		
1	2	2	3	$C = \begin{bmatrix} 3 & 2 & 1 \\ 3 & 1 & 2 \\ 3 & 1 & 2 \end{bmatrix}$	
1	3	1	3		
2	1	3	1		
2	2	1	2	$D = \begin{bmatrix} 3 & 3 & 3 \\ 1 & 2 & 1 \\ 2 & 1 & 2 \end{bmatrix}$	
2	3	2	1		
3	1	3	2		
3	2	1	1	$CD = \begin{bmatrix} 33 & 23 & 13 \\ 31 & 12 & 21 \\ 32 & 11 & 22 \end{bmatrix}$	
3	3	2	2		

discussing such maps appears to be [37], which gives a full classification up to size $N = 3$.

Dual unitary permutation matrices are closely related to known objects from combinatorial designs theory. They can be pictured as certain "broken" or "imperfect" orthogonal arrays or Graeco-Latin squares. The connections are as follows.

Let us list the N^2 quartets (a, b, c, d), where it is understood that for each pair (a, b), we have $(c, d) = U(a, b)$. Dual unitarity means that each quartet can be identified uniquely by specifying either of the following pairs of variables: (a, b), (c, d), (a, c), (b, d). An alternative understanding is found if we compile a table of size $N^2 \times 4$ out of the quartets, such that each row corresponds to a quartet (a, b, c, d). In this table, we find that there are certain pairs of columns, such that in the pair of columns every pair of numbers is present exactly once. This is consistent with the table having N^2 rows. The pairs for which this property holds correspond the pairs of variables (a, b), (c, d), (a, c), and (b, d). Such a table could be regarded as a "broken orthogonal array." The actual orthogonal arrays are similar tables where the uniqueness property would hold for every pair of columns, or more generally, for every subset with a given size k (called the strength of the orthogonal array) [46]. An example for such a broken orthogonal array is shown in Table I for $N = 3$.

The dual unitary permutation matrices can be visualized also in a different way. Let us arrange the values of the functions $c(a, b)$ and $d(a, b)$ in two matrices C and D of size $N \times N$, where the row index is given by a and the column index by b. Such pairs of matrices are generalizations of orthogonal pairs of Latin squares, also called Graeco-Latin squares. A Latin square is a matrix of size $N \times N$ filed with numbers $1, \dots, N$, such that in each row and each column every number is present exactly one time. A pair of Latin squares C and D is called orthogonal, if the pairs of numbers (C_{jk}, D_{jk}) are all distinct. A permutation map U is dual unitary, if the corresponding matrices C and D are orthogonal in the sense we just described, and C is only row-Latin and D is column-Latin.

An example for a dual unitary permutation matrix is shown in Table I. Later in this work, we will use a slightly different, more compact notation: we will combine the matrices C and

D and for better readability we write the pairs of numbers (C_{jk}, D_{jk}) without parenthesis or separation marks.

If a dual unitary permutation matrix is also a perfect tensor, then it corresponds to an actual orthogonal array or equivalently to a pair of orthogonal latin squares. In the theory of combinatorial designs the mutually orthogonal Latin squares (MOLS) are of great interest. A MOLS is a set of Latin squares such that any two of them are orthogonal. There is no complete classification of MOLS, and a recent work treating their enumeration is Ref. [47].

If the map $U(a, b)$ is space reflection invariant, then it means that $D = C^t$ where ^{t} denotes the transpose. In the case of the perfect maps such cases are known as self-orthogonal Latin squares, and it is known that they exist for all N except for 2, 3, and 6 [48]. Space reflection invariant DU maps (which are not necessarily perfect) correspond to self-orthogonal row-Latin squares.

For each permutation map, we can also construct families of quantum gates by adding phases [6], such that

$$U(|a\rangle \otimes |b\rangle) = e^{i\varphi_{cd}}(|c\rangle \otimes |d\rangle),\tag{29}$$

where $c = c(a, b)$ and $d = d(a, b)$ are the classical variables and φ_{cd} stands for a collection of N^2 phases. This is then a generalization of the dressed SWAP gate introduced in Eq. (22).

F. Finite rings

It is well known that orthogonal latin squares can be constructed as linear maps from finite fields; this leads to known constructions for perfect tensors, see, for example, Ref. [19]. Now we generalize this idea to finite rings, in order to construct dual unitary permutation matrix that are not perfect.

Let us consider a finite commutative ring $\mathcal{R}$ of size N and the linear map

$$U(a, b) = (\alpha a + \beta b, \gamma a + \delta b),\tag{30}$$

where $\alpha, \beta, \gamma, \delta \in \mathcal{R}$ are fixed parameters of the map. Even though we view U as a permutation map, it can be represented by a two by two matrix

$$\begin{pmatrix} \alpha & \beta \\ \gamma & \delta \end{pmatrix}.\tag{31}$$

The above permutation map is invertible if the determinant $\alpha\delta - \beta\gamma$ is an invertible element of $\mathcal{R}$. Furthermore the map is DU if β and γ are also invertible elements. The map is perfect if α and δ are also invertible. We are looking for maps which are DU but not perfect.

For example, we consider the ring $\mathbb{Z}_N$ where N is not a prime. Multiplication with a nonzero element $x \in \mathbb{Z}_N$ is invertible, if x is coprime to N. DU maps are then given by linear maps (30) where the three elements β, γ, and $\alpha\delta - \beta\gamma$ are all coprime to N.

Explicit examples are found easily. For example, consider the ring $\mathbb{Z}_N$ for $N = 2k$ such that k is not a multiple of 3; the smallest nontrivial example is $N = 4$. For such N consider the space reflection invariant map

$$U(a, b) = (2a + b, a + 2b).\tag{32}$$

It follows from the considerations above that this map is DU, but it is not perfect. In matrix notation, it is written as

$$\begin{bmatrix} 33 & 41 & 13 & 21 \\ 14 & 22 & 34 & 42 \\ 31 & 43 & 11 & 23 \\ 12 & 24 & 32 & 44 \end{bmatrix},\tag{33}$$

where we identified $0 \equiv 4$.

Perfect tensors are found most easily when the ring is actually a finite field, and $\alpha, \beta, \gamma, \delta$ and $\alpha\delta - \beta\gamma$ are all nonzero. The simplest example for a perfect map is found when the field is $\mathbb{Z}_N$ with some prime $N \geqslant 3$, and the map is

$$U(a, b) = (a + b, a - b).\tag{34}$$

For $N = 3$, this map appeared in the works [6,19,26].

G. Yang-Baxter maps

A special class of dual unitary permutation matrices are those which satisfy the set-theoretical Yang-Baxter relation, which reads

$$U_{12}U_{23}U_{12} = U_{23}U_{12}U_{23}.\tag{35}$$

The relation is understood for operations acting on the triple product X^3, where $X = \{1, 2, \ldots, N\}$. Introduced originally by Drinfeld [49] such maps were studied in detail in the seminal paper [50], and by now the study of Yang-Baxter maps and the associated algebraic structures is a separate topic in mathematics (see for example the influential paper [51]). The dual unitarity condition was called "nondegeneracy" in Ref. [50], and the class of nondegenerate solutions of (35) is the most studied one.

Cellular automata built from Yang-Baxter maps were studied recently in Ref. [52]. It was shown here that these circuits are superintegrable: they possess an exponentially large set of local conserved quantities.

There is no general construction for dual unitary Yang-Baxter maps, but solutions for small N were enumerated in Ref. [53], and they are available online through the associated `github` databases (for sizes $N \leqslant 9$ see Ref. [54]).

H. Graph states

So-called graph states were used in Refs. [21,55,56] to construct perfect tensors. In a concrete representation, we obtain tensors, such that all components have equal magnitude but varying phases, in order to produce maximal entanglement. These ideas can be applied naturally also to DU gates, via the operator-state correspondence. We obtain special complex Hadamard matrices [57], which appear as generalizations of the discrete Fourier transform. A number of examples already appeared in the literature. The DU gate of the kicked Ising model is in this class [3,4,7,11]. Recently generalizations also appeared in Ref. [6] which were called "quantum cat maps." Here we give one slight generalization of the class given in Ref. [6]. We will see that these gates are also related to the permutation maps.

Let us assume that

$$U_{kl}^{ij} = \frac{1}{N}\omega^{F(i,j,k,l)},\tag{36}$$

where ω is the first root of unity given by $\omega = e^{2\pi i/N}$ and $F(i, j, k, l) \in \mathbb{Z}$. It is natural to interpret the variables i, j, k, l and the values of F to be elements of the ring $\mathbb{Z}_N$. We do not assume N to be prime, so $\mathbb{Z}_N$ is not necessarily a field.

We are looking for F functions which are bilinear:

$$F(i, j, k, l) = \alpha_1 ij + \alpha_2 kl + \beta_1 ik + \beta_2 jl + \gamma_1 il + \gamma_2 jk. \tag{37}$$

Linear pieces would correspond to the action of one-site unitaries, therefore we do not add them in this *Ansatz*. The coefficients $\alpha_{1,2}$, $\beta_{1,2}$, and $\gamma_{1,2}$ are also assumed to be elements of $\mathbb{Z}_N$. A bilinear function of this form can be represented by a graph with 4 vertices, and 6 weighted edges between them, such that the weights are given by the coefficients above. Hence the name "graph states."

The unitarity and dual unitarity conditions are

$$\frac{1}{N^2} \sum_{kl} \omega^{F(i,j,k,l)-F(m,n,k,l)} = \delta_{im}\delta_{jn} \tag{38}$$

and

$$\frac{1}{N^2} \sum_{kl} \omega^{F(i,j,k,l)-F(i,m,k,n)} = \delta_{jm}\delta_{ln}. \tag{39}$$

It is our goal to fix the six numerical coefficients $\alpha_{1,2}$, $\beta_{1,2}$, $\gamma_{1,2}$ such that both relations are satisfied. For any $x \in \mathbb{Z}_N$, we have the obvious identity

$$\sum_{k=1}^{N} \omega^{kx} = N\delta_{x,0}. \tag{40}$$

Our goal is to ensure that in the summations above the nonzero terms always correspond to the desired identities.

The unitarity condition holds if the equations

$$\beta_1(i - m) + \gamma_2(j - n) = 0, \quad \gamma_1(i - m) + \beta_2(j - n) = 0 \tag{41}$$

imply $i = m$, $j = n$. The dual unitarity holds if the equations

$$\alpha_1(j - m) + \gamma_1(l - n) = 0, \quad \gamma_2(j - m) + \alpha_2(l - n) = 0 \tag{42}$$

imply $j = m$, $l = n$. This is satisfied in the finite ring $\mathbb{Z}_N$ if the 2×2 matrices corresponding to the equations above are invertible, which means that $\beta_1\beta_2 - \gamma_1\gamma_2$ and $\alpha_1\alpha_2 - \gamma_1\gamma_2$ have to be invertible elements of $\mathbb{Z}_N$ (coprime to N).

Examples are found already for $N = 2$: the self-dual kicked Ising model [3] corresponds to

$$\alpha_1 = \alpha_2 = \beta_1 = \beta_2 = 1, \quad \text{and} \quad \gamma_{1,2} = 0. \tag{43}$$

This choice of parameters gives a DU gate for every N. The corresponding graph state is known in quantum information theory as the cluster state or "C state" [21].

Generalizations of this case called "quantum cap maps" were published in [6]; these solutions also have two parameters equal to zero as in the kicked Ising case. A representative can be chosen as

$$\gamma_1 = \gamma_2 = 0, \quad \alpha_1 = \alpha_2 = \beta_1 = 1, \quad \beta_2 = -1. \tag{44}$$

This is known as the "P state" in quantum information theory [21].

The graph state construction gives a perfect tensor if $\alpha_1\alpha_2 - \beta_1\beta_2$ is also invertible. It is known that the P state

is perfect for every odd N, this follows simply from our requirements. On the other hand, the C state is never perfect.

Let us now consider a special case when $\alpha_1 = \alpha_2 = 0$. In this case the gate is equivalent to a linear map constructed from the finite field $\mathbb{Z}_N$. To see this we use the one-site unitary F, which is the matrix of the discrete Fourier transform given by

$$F_{jk} = \frac{1}{\sqrt{N}} \omega^{-jk}. \tag{45}$$

Computing

$$\tilde{U} = (F \otimes F)U \tag{46}$$

we see that $\tilde{U}$ is a permutation map of the form (30) with a 2×2 matrix given by

$$\begin{pmatrix} \beta_1 & \gamma_1 \\ \gamma_2 & \beta_2 \end{pmatrix}. \tag{47}$$

IV. ERGODICITY OF DU PERMUTATION CIRCUITS

Now we consider the ergodicity properties of the circuits built from DU permutation maps. In this section, we focus on DU gates which are not perfect maps; perfect permutation maps will be considered separately in the next section.

We analyze the in-equivalent circuits for small local dimensions $N = 2$ and 3. We consider two physical properties of these systems: the number of local conserved charges as a function of the range of the charge density, and the orbit lengths in the corresponding classical cellular automaton. Before turning to the concrete examples let us first discuss these two properties.

It was already in explained in Sec. II A that in DU circuits all conserved charges are gliders: the time evolution of the charge densities is a mere translation to the left or to the right with constant speed, without any operator spreading. In most previous works, the ergodicity of the DU circuits was characterized based on the one-site density matrices: it was implicitly stated that a DU circuit is nonergodic iff there is at least one one-site glider. At the same time, it was mentioned in Ref. [5] that there can be models where the one-site density matrices are fully chaotic, but gliders can appear within the Hilbert spaces of the multisite operators (see also the so-called "still gliders" wilt multisite support found in Ref. [38]). In this work, we show concrete examples for this behavior.

It was also mentioned in Sec. II, that if a DU circuit has at least one conserved charge, then it has infinitely many. In such a case a relevant question is, whether there are additional gliders at longer range which are algebraically independent from products of shorter gliders. As far as we know this question has not yet been investigated in the integrable DU circuits. Partial results are found in the work [52], which treated DU circuits from Yang-Baxter maps. In these models, an exponentially large set of gliders was constructed, such that the multi site gliders are indeed operator products of the three-site gliders (this was not explicitly stated in Ref. [52] but it is clear from the construction). However, even in these cases, it is not clear whether there are always one-site gliders, or additional charges on top of those following from the Yang-Baxter structure.

Below we collect some numerical data about the number of gliders for various models and operator lengths. The number of gliders with a maximal range $2\alpha - 1$ can be found most easily by looking at the eigenvalues of the transfer matrix t_α written earlier in (15). We numerically diagonalize the t_α for various permutation circuits and ranges $\alpha \leqslant 4$. Each time we publish the number of eigenvalues which are unity or roots of unity, subtracting the trivial case corresponding to the identity operator. The algebraic independence of these operators is a separate question, which should be investigated on a case by case basis; below we just publish the overall numbers and the conclusions that can be drawn from this.

Besides the existence of gliders the other physical property we look at is the average length of the orbits in the dual unitary permutation matrices in a finite volume L (for similar earlier studies see for example [52,58,59]). If $|\Psi\rangle$ is a product state in the local basis, then the set of product states $|\Psi(t)\rangle$, $t = 0, 1, 2 \ldots$ is called the orbit of $|\Psi\rangle$. The time evolution is invertible, and the configuration space is finite for finite L, therefore all orbits are periodic, and we say $n > 0$ is the orbit length of the product state $|\Psi\rangle$ if it is the smallest number n such that $|\Psi(2n)\rangle = |\Psi(0)\rangle$. We included a factor of 2 in this definition, because the Floquet cycle has period 2, and orbits can be defined only for completions of a Floquet cycle. We define $\bar{n}$ as the average orbit length computed over all states of the system.

In the numerical computations, the observed average orbit lengths are only approximations of the true value, because for larger volumes it is not possible to cover the complete configuration space. Therefore our numerical method was the following: we computed the orbit lengths for 200 randomly chosen initial configurations, and computed the average. In order to test the accuracy of these results, we run multiple ($\simeq 10$) instances of these averaging procedures and computed the variance of the results obtained. Whenever we performed these checks we found a variance of less than 3% in the average on logarithmic scale.

The orbit lengths carry information about the global ergodicity properties of these deterministic circuits. In the most ergodic cases, the average orbit lengths grow together with the dimension of the Hilbert space. In such a case, $\bar{n} \sim N^L$: this means that there are a few giant orbits (or possibly just a single giant orbit) covering a finite fraction of the configuration space, with the rest covered by smaller orbits. On the other hand, conserved charges foliate the configuration space, and this leads to shorter orbit lengths. Therefore we expect that the number of gliders should be reflected in the average orbit lengths.

During the enumeration of the models we consider two circuits to be equivalent if their two-site gates are related to each other by combinations of time or space reflection, and the diagonal similarity transformations (20).

A. $N = 2$

For $N = 2$, there are five nonequivalent DU permutation circuits. Three of them are noninteracting: they are $U = \mathcal{P}$,

TABLE II. Total number of nontrivial gliders for a given range, for six selected models at $N = 3$. The table shows the number of eigenvalues $|\lambda| = 1$ of the transfer matrices t_α plus the same number for the space reflected version, minus the two trivial eigenvalues corresponding to the identity matrices. We did not check the algebraic independence of the gliders.

α	1	2	3	4
C_1, C_2	0	0	0	0
I_1	4	40	364	3280
I_2	8	80	728	6560
E_1	0	2	11	54
E_2	0	0	1	3

$U = \sigma_1^x \mathcal{P}$ and $U = \sigma_1^x \sigma_2^x \mathcal{P}$. The remaining two cases are

$$U_1 = \begin{bmatrix} 12 & 21 \\ 11 & 22 \end{bmatrix} \quad \text{and} \quad U_2 = \begin{bmatrix} 21 & 12 \\ 22 & 11 \end{bmatrix}. \quad (48)$$

Here we used the matrix notation explained in Sec. III E.

These gates can be understood as combinations of the CNOT and SWAP gates, and also a single site spin flip. Both models have one left moving and right moving glider already for range $\alpha = 1$, so they are not ergodic. A direct check of Eq. (35) shows that U_1 and U_2 are not Yang-Baxter maps, nevertheless they appear integrable: the orbit lengths are found to be at most linear in L in both models.

B. $N = 3$

Dual unitary permutation matrices with $N = 3$ offer more possibilities and some surprises. For $N = 3$, we performed a brute force computer search and found 227 nonequivalent models. Each one of the 227 models can be connected to one of the 18 biunitary permutations found in Ref. [37], by adding a SWAP gate and further one-site permutations. However, the single permutations can drastically change the physical properties of the circuits. These permutation matrices were already investigated in the paper [6], which considered the various possibilities for the entangling power and the behavior for the one-site operators. Our contribution is that we consider the higher charges and the orbit lengths of the resulting circuits.

We computed the numbers of gliders with ranges $\alpha = 1, 2, 3,$ and 4 for all 227 models, and for a selected set of models, we also considered the orbit lengths. For most models, we observed the expected behavior, that the information gained from the one-site operators completely determines the physical behavior. However, for a smaller number of models, we also found some surprises: Sometimes the models do not have any gliders for $\alpha = 1$ or even $\alpha = 2$, but gliders start to appear at longer ranges. As far as we know, this has not yet been observed in the literature.

Regarding orbit lengths we observed the expected behavior: as a rule of thumb, the more charges a model has, the shorter its classical orbits are.

Publishing the data corresponding to all 227 models seems pointless, instead we focus on concrete examples. The numbers of gliders are summarized in Table II, and the orbit lengths are discussed in the text.
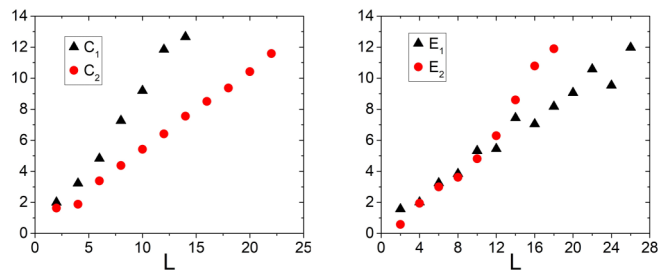
FIG. 4. Average orbit lengths for four selected models; we plotted $\log_3 \bar{n}$ as a function of the volume. The labels of the models correspond to the matrices given in the main text.

As first ergodic examples, we consider the models given by

$$C_1 = \begin{bmatrix} 32 & 22 & 13 \\ 23 & 33 & 12 \\ 21 & 31 & 11 \end{bmatrix} \quad \text{and} \quad C_2 = \begin{bmatrix} 13 & 23 & 33 \\ 31 & 12 & 22 \\ 32 & 21 & 11 \end{bmatrix}.$$
(49)

Neither of these two models has any glider up to range $\alpha = 4$. The orbit lengths grow as $\bar{n} \approx 3^L$ and $\bar{n} \approx 3^{L/2}$, for C_1 and C_2, respectively; they are plotted in Fig. 4 on a logarithmic scale.

The model C_1 is as close to perfectly ergodic as possible: for each L, we find one giant orbit, covering a finite fraction of the configuration space, and a number of shorter orbits. For C_2, we find that the average orbit lengths scale with the square root of the size of the Hilbert space: this decrease could be a result of a hidden discrete symmetry, but we did not find an explanation yet.

As examples for integrable cases we present the following two maps:

$$I_1 = \begin{bmatrix} 11 & 31 & 21 \\ 12 & 23 & 33 \\ 13 & 22 & 32 \end{bmatrix} \quad \text{and} \quad I_2 = \begin{bmatrix} 11 & 21 & 31 \\ 12 & 32 & 22 \\ 13 & 23 & 33 \end{bmatrix}.$$
(50)

Both maps are interacting: they have nonzero entangling power. For the average orbit lengths, we find $\bar{n} \approx L$; also the maximal orbit length is found to increase only linearly with the volume. Direct computation shows that I_1 is a Yang-Baxter map, this explains its integrability [52]. I_2 is not a Yang-Baxter map, but it has a very simple structure: it is a controlled unitary, which we write as

$$I_2 = \mathcal{P}\left[P_1^{(1)}M_2 + P_1^{(2)} + P_1^{(3)}\right], \quad M = \begin{pmatrix} 0 & 0 & 1 \\ 0 & 1 & 0 \\ 1 & 0 & 0 \end{pmatrix}.$$
(51)

Here the one-site projectors are as before $P^{(j)} = |j\rangle\langle j|$ and M is one-site permutation matrix. The maximal number of gliders for $\alpha = 1$ is $2(N^2 - 1)$ and it appears that I_2 has half of them, and I_1 has a quarter of them.

We also found a total number of 30 nonequivalent circuits which have no gliders at range $\alpha = 1$ but a varying number of gliders for $\alpha = 2$. None of these gates is a Yang-Baxter map. In addition, we found three nonequivalent circuits that have no gliders for $\alpha = 1, 2$ but a single glider for $\alpha = 3$. Examples for models with gliders appearing at $\alpha = 2$ and $\alpha = 3$ are

given by

$$E_1 = \begin{bmatrix} 32 & 22 & 13 \\ 31 & 21 & 12 \\ 23 & 33 & 11 \end{bmatrix} \quad \text{and} \quad E_2 = \begin{bmatrix} 11 & 32 & 21 \\ 33 & 13 & 23 \\ 12 & 31 & 22 \end{bmatrix}.$$
(52)

For E_1, we find a total number of 2 gliders for $\alpha = 2$ (both are right-moving), and for E_2 we have a single glider with $\alpha = 3$. The growth of the orbit lengths in these models is plotted on Fig. 4, again in logarithmic scale. For E_1, we see a clear exponential growth, with a noninteger exponent. Data on E_2 are less clear, and likely larger volumes would be needed to establish the growth exponent.

The models given by E_1 and E_2 should be called "integrable," because after all they have an infinite set of gliders. The algebraic reason for their integrability is not known at the moment. Whether or not integrability is truly "accidental" here, or whether there a deeper reason behind it, is a question for further research.

V. ERGODICITY PROPERTIES OF DU CIRCUITS WITH PERFECT MAPS

In this section, we investigate circuits with perfect permutation maps for $N = 3$, 4, and 5. As discussed above, such maps correspond to orthogonal Latin squares. As quantum gates they are perfect tensors and they have maximal entangling power. As discussed in Ref. [6] they are maximally chaotic on the level of local correlation functions. Furthermore, they are strong scramblers: the perfect property can be used to analytically prove the maximal operator spreading [19].

The work [19] considered the perfect map given by (34), which is a linear map over finite fields. At the first sight this linearity has nothing to do with the ergodicity of the resulting quantum circuit: the map is a perfect tensor, and the circuit is locally maximally chaotic. Nevertheless, it was observed in Ref. [19] that there are global signs of the integrability: the recurrence time of the system shows unexpected behavior. We discuss this phenomenon in detail.

The recurrence time T of the deterministic circuit is defined as the smallest nonzero integer such that $|\Psi(2T)\rangle = |\Psi(0)\rangle$ for all initial states $|\Psi(0)\rangle$. T is the least common multiple of the orbit lengths, and it is the classical analog of the Poincaré recurrence time. For ergodic systems, T is expected to grow doubly exponentially [19]. On the other hand, it is known that in some integrable models it grows only polynomially. For example, in the case of dual unitary Yang-Baxter maps, we have $T = L/2$, and for other Yang-Baxter maps, quadratic or cubic growth was also demonstrated in Ref. [52].

It was noticed in Ref. [19] that for the perfect tensor map (34) over $\mathbb{Z}_3$, the recurrence time T grows at most exponentially with the volume, however, T shows a very irregular behavior, depending very strongly on the prime factorization of the number L. It was noted in Ref. [19] that for volumes $L = 2 \cdot 3^m$ with some $m = 1, 2, \ldots$ the growth is linear: $T = 2L$, but for other values $L = 2q$ with some prime q it grows exponentially with an unknown exponent. Numerical data for the recurrence times is presented in Table III, and

TABLE III. Recurrence times in the linear model over $\mathbb{Z}_3$ for small values of L.

L	2	4	6	8	10	12	14	16	18	20	22	24	26	28	30
T	4	4	12	12	20	12	52	60	36	40	244	36	364	364	60

L	32	34	36	38	40	42	44	46	48
T	240	820	36	1036	4920	156	244	354292	180

for completeness we also plot in Fig. 5. We can see certain values of L where T appears to be growing exponentially, just to be followed by other values of L with unexpectedly small recurrence times. This behavior is in stark contrast with the maximal ergodicity seen in the local quantities.

The determination of the function $T(L)$ is an interesting question on its own, which can be formulated as a problem in linear algebra over finite fields. More generally, let us choose a prime $N = p \geqslant 3$ and consider the vector space $(\mathbb{Z}_p)^L$ with some even volume L. Consider the linear map

$$U(a, b) = (a + b, a - b) \tag{53}$$

over $(\mathbb{Z}_p)^2$. The extension to a Floquet circuit gives the update rule $\mathcal{V}$, which can be represented as a linear operator acting on this vector space:

$$\mathcal{V} = AB. \tag{54}$$

Here A is the block diagonal matrix

$$A = \begin{pmatrix} 1 & 1 & & & \\ 1 & -1 & & & \\ & & \ddots & & \\ & & & 1 & 1 \\ & & & 1 & -1 \end{pmatrix} \tag{55}$$

and $B = CAC^{-1}$ with C being the cyclic shift operator on $(\mathbb{Z}_p)^L$. The matrices are of size $L \times L$ with elements in $\mathbb{Z}_p$. The order of the product in (54) is actually different from the choice of (4), but this does not change the physical properties, and it is chosen to conform with the conventions of Appendix.

The recurrence time T is defined as the smallest nonzero integer such that

$$\mathcal{V}^T = 1 \tag{56}$$

as a matrix over $(\mathbb{Z}_p)^L$.

FIG. 5. (Left) Exact recurrence times of the linear model over $\mathbb{Z}_3$; this is the plot of $\log_3(T(L))$ with $T(L)$ presented in Table III. (Right) Average orbit lengths for two models at $N = 5$: the linear model given by V_1 and the dressed model given by V_2. We plotted $\log_5(\bar{n})$, and for V_2, we observe a linear function with slope ≈ 1, thus the model is maximally ergodic.

The determination of $T(L)$ (together with an actual solution of the time evolution) requires the use of the Fourier transform over extensions of the finite field $\mathbb{Z}_p$. This is treated as a separate problem in Appendix, written by Roland Bacher and Denis Serre. Appendix includes a rigorous proof of the linear growth of $T(L)$ for $L = 2p^m$ and it is also proven that the maximal growth of $T(L)$ is only exponential in L.

Both the theoretical treatment and also the numerical data show that these linear maps behave essentially the same way for all p. Furthermore, it is not at all crucial which linear map we choose, as long as it is a perfect map: there can be some differences in the actual values of $T(L)$, but the overall characteristics are the same. Furthermore, essentially the same behavior is also seen if the perfect map is linear over a finite field of order p^m with some $m > 2$.

The global nonergodicity and the solvability are consequences of the linearity of the map, but strangely this is seen only at the "classical level," and the local indicators of quantum chaos are signaling completely nonergodic behaviour. The observed phenomenon is very similar to the behavior of the discrete version of Arnold's cat map, whose recurrence time was studied long time ago by Dyson and Falk [60].

It was already suggested in Ref. [19] that a truly ergodic perfect quantum circuit could be constructed if the linear maps are dressed with one-site unitaries, for example, with some rotations with nonrational parameters. We considered this idea within the class of dual unitary permutation matrices: we added one-site permutations to the outgoing legs of the linear map, and investigated the orbit lengths of the circuit thus obtained. For $N = 3$, this idea does not give anything new, because every permutation of three elements can be described by a linear function in $\mathbb{Z}_3$, thus dressing with one-site permutations would not give a nonlinear map. Instead, we considered the next prime $N = 5$ and the maps

$$\tilde{U} = (S_1 \otimes S_2)U, \tag{57}$$

where U is the same linear map (53) as before, but S_1 and S_2 are permutations that are not linear maps in $\mathbb{Z}_5$. We observed the expected behavior: the addition of just one "nonlinear" permutation is enough to guarantee full ergodicity.

To be concrete, let us consider the map (53) over $\mathbb{Z}_5$, represented by the matrix

$$V_1 = \begin{bmatrix} 11 & 25 & 34 & 43 & 52 \\ 22 & 31 & 45 & 54 & 13 \\ 33 & 42 & 51 & 15 & 24 \\ 44 & 53 & 12 & 21 & 35 \\ 55 & 14 & 23 & 32 & 41 \end{bmatrix}. \tag{58}$$

Here we chose a convention so that the pair $(1,1)$ is kept invariant (vacuum configuration), so that the elements $0, \ldots, 4 \in \mathbb{Z}_5$ correspond to our basis states $|1\rangle, |2\rangle, \ldots, |5\rangle$ in this

order. Let us now consider the permutation S given by $(1, 2, 3, 4, 5) \rightarrow (1, 5, 3, 2, 4)$. It is easy to check that this permutation is not a linear map over $\mathbb{Z}_5$. Now we perform this permutation on the first outgoing variable of V_1 according to (57). This leads to the matrix

$$V_2 = \begin{bmatrix} 11 & 55 & 34 & 23 & 42 \\ 52 & 31 & 25 & 44 & 13 \\ 33 & 22 & 41 & 15 & 54 \\ 24 & 43 & 12 & 51 & 35 \\ 45 & 14 & 53 & 32 & 21 \end{bmatrix}. \quad (59)$$

The average orbit lengths for the models given by V_1 and V_2 are plotted in Fig. 5. For V_1, we observe the same pattern as earlier for the linear map: the orbit lengths depend crucially on the prime factorization of the volume, and the recurrence time grows only exponentially. For V_2, on the other hand, we see the expected maximal ergodicity: the average orbit lengths grow approximately as 5^L.

For completeness, we also considered perfect maps that have absolutely no relation with finite fields. It is known that the smallest local dimension at which such a map appears is $N = 7$, in which case there are six nonequivalent perfect maps such that only one of them is related to $\mathbb{Z}_7$ and the other five are unrelated [47,61]. An example for such an unrelated map is given by [61]

$$U = \begin{bmatrix} 11 & 22 & 33 & 44 & 55 & 66 & 77 \\ 24 & 16 & 41 & 35 & 67 & 73 & 52 \\ 36 & 45 & 12 & 23 & 71 & 57 & 64 \\ 47 & 51 & 65 & 72 & 26 & 34 & 13 \\ 53 & 37 & 76 & 61 & 14 & 42 & 25 \\ 62 & 74 & 27 & 56 & 43 & 15 & 31 \\ 75 & 63 & 54 & 17 & 32 & 21 & 46 \end{bmatrix}. \quad (60)$$

In this case, we also observed complete ergodicity: for the small volumes accessible to numerical treatment, we observed orbit lengths comparable to 7^L.

VI. DISCUSSION

In this work, we studied the dynamics of the DU circuits with permutation maps, and discussed two unexpected phenomena. (1) There are models, where conserved charges appear only for multisite operators [concrete examples were given by the matrices E_1 and E_2 in (52)]. (2) There are models, which appear maximally chaotic when looking at the local quantum mechanical behavior, whereas they appear in fact integrable/solvable if good classical coordinates are chosen (these are the DU gates obtained from the linear maps, see Sec. V). Both phenomena tell us that caution needs to be exercised when classifying quantum cellular automata based on the common indicators of quantum chaos.

It would be important to see, whether these two phenomena are restricted to permutation maps, or perhaps they also appear for genuinely quantum mechanical DU gates. The short recurrence times are most likely restricted to the circuits that have close relations with the linear maps (over fields or rings). On the other hand, circuits with only multisite gliders could exist outside the realm of permutation maps, although it seems difficult to find other examples.

The reader might wonder, why did we restrict ourselves to DU gates, and why do not we perform similar searches among models with arbitrary permutation maps. There were two motivations for focusing only on the DU circuits. On the one hand side, in these models all conserved charges are gliders, and this makes the search for the charges especially simple. On the other hand, these models (and their generalizations to multileg tensors, perfect or imperfect) are relevant for the study of quantum scrambling and also for holography. Therefore information about these circuits could be useful for other studies as well.

The linear maps that we treated appear to be at a strange intersection of integrability and chaos. The general idea in physics is that linearity implies solvability, which is a counterpart of chaos. However, in these models, some indicators of quantum chaos signal complete ergodicity, at least for the local quantities. The behavior is very similar to the discrete version of Arnold's cat map, see Ref. [60].

In these linear models we have linearity in the classical variables over finite fields or rings. Therefore the mathematical solvability is much more delicate than usually and it has some surprises (see Appendix). Linear maps over finite fields or rings were discussed earlier (see, for example, Refs. [50,62]), but we did not find in the literature a proper solution of the circuits considered in this work. We believe it would be worthwhile to consider the linear models in more detail, including those which involve rings but not fields.

Furthermore, it would be interesting to study the entanglement growth in the DU permutation models, in relation with the number of gliders and the growth of the orbit lengths. Also, it would be important to find exact solutions for quenches in the special models we considered, in analogy with the earlier work [10]. Such studies could highlight the role of longer gliders in the emerging steady states. What type of generalized Gibbs ensemble do these models equilibrate to? This is an interesting open question at the moment.

In the present work, we only focused on dual unitary circuits, but much of this material could be applied also to the triunitary circuits introduced in Ref. [31]. Both the constructions for the gates, and the studies of the ergodicity could be applied to these circuits. The integrability properties of triunitary gates have not yet been investigated, and it would be interesting to consider Yang-Baxter structures also for those models.

APPENDIX: THE RECURRENCE TIME OF THE LINEAR CELLULAR AUTOMATA

In this Appendix, we treat the question posed in Sec. V: what is the recurrence time in the circuit given by the perfect map (53)? This is equivalent to finding the order of the matrix $\mathcal{V}$ (54) modulo p. The problem requires the use of Fourier transform over finite fields.

For a reason that will become clear soon after, we use the standard notation $\mathbb{F}_p = \mathbb{Z}/p\mathbb{Z}$ for the field with p elements. Let $\mathbf{M}_L(\mathbb{F}_p)$ stand for the ring of matrices of size $L \times L$ with coefficients in $\mathbb{F}_p$. Linear algebra in $\mathbf{M}_L(\mathbb{F}_p)$ follows essentially the same rules as in $\mathbf{M}_L(\mathbb{R})$ or $\mathbf{M}_L(\mathbb{C})$. Mind however that $\mathbb{C}$ is algebraically closed (every polynomial $P \in \mathbb{C}[X]$ splits over $\mathbb{C}$) but finite fields are not.

1. Finite fields

In a finite field K, the sum $1 + \cdots + 1$ vanishes when the number of summands is a multiple of some number p, a prime number called the *characteristic*. For all $a \in K$, $pa = a + \cdots + a = 0$. The field can be viewed as a vector space over $\mathbb{F}_p$. Denoting its dimension n, its cardinal is thus p^n. A sound fact is that, given $n \geqslant 1$, there exists one and only one field with $q = p^n$ elements, up to isomorphism. Denoted $\mathbb{F}_q$, it can be seen as the splitting field of the polynomial $X^q - X$: it is the smallest field containing $\mathbb{F}_p$ over which the given polynomial completely factorizes. Its multiplicative group $\mathbb{F}_q^\times$ is thus the set of $(q-1)$th roots of unity. Contrary to the complex case, roots of unity cannot be expressed as exponentials, since an exponential function cannot be defined in characteristic p.

When $q = p^n$ and $q' = p^m$, $\mathbb{F}_q$ is contained in $\mathbb{F}_{q'}$ if and only if $n|m$ (n divides m); we say that $\mathbb{F}_{q'}$ is an *extension* of $\mathbb{F}_q$, of degree m/n. More generally $\mathbb{F}_q \cap \mathbb{F}_{q'} = \mathbb{F}_r$, where $r = p^{\gcd(n,m)}$ and $\mathbb{F}_q \cdot \mathbb{F}_{q'} = \mathbb{F}_s$ where $s = p^{\text{lcm}(n,m)}$.

Let $\ell \geqslant 2$ be an integer. Contrary to the complex case, there do not always exist ℓ distinct ℓth roots of unity. For instance, 1 is the only pth root of unity in every extension of $\mathbb{F}_p$! However, if $p \nmid \ell$ (p does not divide ℓ), then there exist ℓ distinct ℓth roots of unity. They belong to $\mathbb{F}_q$ where $q = p^n$ and n is the smallest nonzero number such that $\ell|p^n - 1$. In other words, $p^n \equiv 1 \bmod \ell$; n is the order of p in the group $(\mathbb{Z}/\ell\mathbb{Z})^\times$ of invertible elements of $\mathbb{Z}/\ell\mathbb{Z}$. These roots form a multiplicative group denoted U_ℓ.

2. Fourier analysis of $\mathcal{V}$

Let $L = 2\ell$ be an even integer and p be an odd prime number. We form the matrix $\mathcal{V} = AB$ as given by (54) and the problem is to evaluate the order $o_p(L)$ of $\mathcal{V}$ in $\mathbf{GL}_L(\mathbb{F}_p)$. For this, we decompose vectors $x \in F^L$ into an odd and an even part: $y = (x_1, x_3, \ldots, x_{L-1})$ and $z = (x_2, x_4, \ldots, x_L)$, both in $\mathbb{F}^\ell$. The images $x' = Ax$ and $x'' = Bx$ are given by

$$y'_j = y_j + z_j, \quad z'_j = y_j - z_j,$$

and

$$y''_j = -y_j + z_{j-1}, \quad z''_j = y_{j+1} + z_j,$$

where the indices are understood mod ℓ. The vector $X = \mathcal{V}x$ is thus obtained through

$$Y_j = y_{j-1} - y_j - z_{j-1} - z_j, \quad Z_j = y_j + y_{j+1} - z_j + z_{j+1}. \tag{A1}$$

Let C be the cyclic shift operator acting on L variables. The matrix $\mathcal{V}$ commutes with C^2: it is invariant with respect to translations of two sites.

Now our idea is to perform a Fourier transformation, to make use of this translational invariance. The standard step would be to construct the eigenspaces of C^2 and to diagonalize the matrix $\mathcal{V}$ within these eigenspaces. However, as opposed to the case of the complex numbers, the Fourier transform can not always be performed. Sometimes there are not enough distinct eigenvalues of C^2 (which are roots of unity), furthermore, C^2 is not always diagonalizable.

We set $L = 2l$ and work over a field $\mathbb{F}$, and also use the notation $C_\ell = C^2$. The matrix $\mathcal{V}$ operates on the direct sum $\mathbb{F}[C_\ell] \oplus \mathbb{F}[C_\ell]$ of two copies of the group algebra $\mathbb{F}[C_\ell]$ of the cyclic group $\mathbb{Z}/\ell\mathbb{Z}$; the two copies correspond to the odd and even parts of $c \in \mathbb{F}^L$ introduced above. The action of $\mathcal{V}$ commutes with the obvious diagonal action of C_ℓ on both copies (corresponding to odd and even indices).

Observe that $\mathbb{F}[G_1 \times G_2] = \mathbb{F}[G_1] \otimes_\mathbb{F} \mathbb{F}[G_2]$. The order of $\mathcal{V}$ over a finite field $\mathbb{F} = \mathbb{F}_p$ is thus (up to a small factor given by a divisor of $p - 1$) the least common multiple of the order of $\mathcal{V}(2a)$ and $\mathcal{V}(2b)$ over k, where $\ell = ab$ with a and b coprime. For understanding the order of $\mathcal{V}(L)$ over an odd prime p, it is thus essentially enough to understand the cases $L = 2p^m$ and L coprime to p.

Below we will treat the two cases separately. The general strategy is the same in both cases: understanding the invariant subspaces for the action of C^2, and diagonalizing M within these subspaces. However, the details of the computations will be different.

3. The case $L = 2p^m$

We consider now the case $\ell = p^m$ over the finite primary field $\mathbb{F}_p$ for an odd prime p. We have $\mathbb{F}_p[\mathbb{Z}/p^m\mathbb{Z}] = \mathbb{F}_p[t]/(1 - t^{p^m}) = \mathbb{F}_p[t]/(1 - t)^{p^m}$. A generator of the cyclic group $\mathbb{Z}/p^m\mathbb{Z}$ acts thus on $\mathbb{F}_p[\mathbb{Z}/p^m\mathbb{Z}]$ by a unique Jordan-block J of eigenvalue 1 and maximal size p^m. We denote by $T = J - \text{Id}$ the associated nilpotent linear operator. The obvious actions of $T \oplus T$ and $\mathcal{V}$ on $\mathbb{F}_p[\mathbb{Z}/p^m\mathbb{Z}] \oplus \mathbb{F}_p[\mathbb{Z}/p^m\mathbb{Z}]$ commute. The kernel of $T \oplus T$ has dimension 2 and it consists of those vectors where both the odd and even parts are constants. Diagonalization of $\mathcal{V}$ within this sub-space gives two eigenvectors with eigenvalues $\lambda_\pm = \pm 2\sqrt{-1}$, which are elements of $\mathbb{F}_p$ or its extension $\mathbb{F}_{p^2}$, solving the equation $\lambda^2 + 4 = 0$.

Let v be an arbitrary eigenvector of $\mathcal{V}$. A suitable power of the nilpotent operator $T \oplus T$ sends v onto a nonzero element of $\ker(T \oplus T)$. This implies that v is also of eigenvalue $\pm 2\sqrt{-1}$. The matrix $\mathcal{V}^2$ is thus a union of Jordan-blocks with common eigenvalue -4. Since we are working in characteristic p, the matrix $\mathcal{V}^{2p^m}$ is a nonzero multiple of the identity.

Corollary A.1. The order of $\mathcal{V}$ over the finite field $\mathbb{F}_p$ equals thus ap^μ for some $\mu \leqslant m$ where a is the twice the order of -4 in the multiplicative group $(\mathbb{Z}/p\mathbb{Z})^\times$.

We have thus proven that for the values $L = 2p^m$ the order of $\mathcal{V}$ grows at most linearly with L. This is a new result of this Appendix; the linear growth was stated in Ref. [19], but a mathematical proof was not provided there.

The exponent μ occurring in the order is in $\{m - 2, m - 1, m\}$ since the matrix $\mathcal{V}(L)$ is "concentrated" near the identity. More precisely, $\mathcal{V}(L)e_i$ is a linear combination with coefficients in $\{0, \pm 1\}$ involving only $e_{i-2}, \ldots, e_{i+2}$ (with indices read modulo p^m). Moreover, e_{i-1} and e_{i+1} are involved with nonzero coefficients. This implies that $\mathcal{V}(L)$ has order at least $L/4$ over any finite field. We have thus $2(p-1)p^{\mu} \geqslant p^m/2$ implying $\mu \geqslant m - 2$.

4. The case ℓ coprime to p

Let us now consider the case when ℓ is not divisible by p. In such a case, there exist enough roots of unities, and the shift operator C_ℓ is diagonalizable. Therefore this case is closer in spirit to the usual Fourier transform known from linear systems over the complex numbers.

Given an ℓth root of unity ω, we define a vector $v_\omega = (1, \omega, \ldots, \omega^{\ell-1})$. If $U_\ell \subset \mathbb{F}_q$, then the vectors v_ω, as $\omega \in U_\ell$, form a basis $\mathcal{B}$ of $(\mathbb{F}_q)^\ell$. The change of coordinates from the canonical basis to $\mathcal{B}$ is the discrete Fourier transform. We have the decomposition $(\mathbb{F}_q)^L = \oplus_{\omega \in U_\ell} E_\omega$ where E_ω is the plane defined by $y, z \parallel v_\omega$. If $y = a v_\omega$ and $z = b v_\omega$, then (A1) yields $Y = \alpha v_\omega$ and $Z = \beta v_\omega$ with

$$\begin{pmatrix} \alpha \\ \beta \end{pmatrix} = \mathcal{V}(\omega) \begin{pmatrix} a \\ b \end{pmatrix}, \quad \mathcal{V}(\omega) = \begin{pmatrix} \omega^{-1} - 1 & -\omega^{-1} - 1 \\ \omega + 1 & \omega - 1 \end{pmatrix}.$$

The matrix $\mathcal{V}$ is thus conjugated to the block-diagonal matrix $\mathcal{V}'$ whose diagonal blocks are the $\mathcal{V}(\omega)$'s. In particular, its order is the lcm of the orders of the blocks in $\mathbf{GL}_2(\mathbb{F})$. Remark that $\mathcal{V}(\omega)$ and $\mathcal{V}(\omega^{-1})$ are conjugated to each other.

The characteristic polynomial of $\mathcal{V}(\omega)$ is $\lambda^2 + (2 - \omega - \omega^{-1})\lambda + 4$. It admits disctinct roots provided $\omega \neq -1$ and $\omega + \omega^{-1} \neq 6$. If so, $\mathcal{V}(\omega)$ is diagonalizable and its order is the lcm of the order of its eigenvalues. The order of $\mathcal{V}(-1) = -2I_2$ is just the order of -2 in $\mathbb{F}_p$. If $\omega + \omega^{-1} = 6$, then $\mathcal{V}(\omega)$ is not diagonalizable and its double eigenvalue is $\lambda = 2$; its order is p times the order of 2 in $\mathbb{F}_p$.

Denote n the order of p mod ℓ, and $q = p^n$ so that $U_\ell \subset \mathbb{F}_q$. One can prove that $\omega + \omega^{-1}$ belongs to $\mathbb{F}_{p^s}$ with $s = n$ if n is odd, or $s = n/2$ if n is even. Since the eigenvalues of $\mathcal{V}(\omega)$ obey a quadratic equation with coefficients in $\mathbb{F}_{p^s}$, they belong to $\mathbb{F}_{p^{2s}}$. In particular, their order divides $p^{2s} - 1$. We conclude that $o_p(L)$ divides $\mathrm{lcm}(p(p-1), p^{2s} - 1)$, hence

Proposition A.1. The order of $\mathcal{V}$ divides $p(p^{2s} - 1)$, hence $p(p^{2n} - 1)$.

Since n divides the order $\phi(\ell)$ of the group $(\mathbb{Z}/\ell\mathbb{Z})^\times$ (ϕ is Euler totient function) and $\phi(\ell) \leqslant \ell - 1$ (with equality if ℓ is prime), we infer the exponential bound.

Corollary A.2. We have $o_p(L) \leqslant p^{L-1} - p$.

With this we have obtained a rigorous upper bound for the exponential growth.

5. The case of p-repunits: quadratic growth.

The exponential bound is much too big in some cases. For example, let us consider the case where $\ell = p_n := \frac{p^n - 1}{p - 1}$ (called a p-repunit because it writes $1 \cdots 1$ in base p). The letter n is chosen on purpose: it is the order of p mod ℓ. Then proposition (A1) gives a quadratic bound

$$o_p(L) \leqslant p[((p-1)\ell + 1)^2 - 1] = p(p-1)\ell((p-1)\ell + 1).$$

This subset of volumes with quadratic growth was not noticed in Ref. [19].

---

[1] J.-S. Caux and J. Mossel, Remarks on the notion of quantum integrability, J. Stat. Mech. (2011) P02023.

[2] F. H. L. Essler and M. Fagotti, Quench dynamics and relaxation in isolated integrable quantum spin chains, J. Stat. Mech. (2016) 064002.

[3] B. Bertini, P. Kos, and T. Prosen, Exact Spectral Form Factor in a Minimal Model of Many-Body Quantum Chaos, Phys. Rev. Lett. **121**, 264101 (2018).

[4] B. Bertini, P. Kos, and T. Prosen, Entanglement Spreading in a Minimal Model of Maximal Many-Body Quantum Chaos, Phys. Rev. X **9**, 021033 (2019).

[5] B. Bertini, P. Kos, and T. Prosen, Exact Correlation Functions for Dual-Unitary Lattice Models in 1+1 Dimensions, Phys. Rev. Lett. **123**, 210601(2019).

[6] S. Aravinda, S. A. Rather, and A. Lakshminarayan, From dual-unitary to quantum Bernoulli circuits: Role of the entangling power in constructing a quantum ergodic hierarchy, Phys. Rev. Research **3**, 043034 (2021).

[7] S. Gopalakrishnan and A. Lamacraft, Unitary circuits of finite depth and infinite width from quantum channels, Phys. Rev. B **100**, 064309 (2019).

[8] B. Bertini, P. Kos, and T. Prosen, Operator Entanglement in Local Quantum Circuits I: Chaotic Dual-Unitary Circuits, SciPost Phys. **8**, 067 (2020).

[9] B. Bertini, P. Kos, and T. Prosen, Operator Entanglement in Local Quantum Circuits II: Solitons in Chains of Qubits, SciPost Phys. **8**, 068 (2020).

[10] L. Piroli, B. Bertini, J. I. Cirac, and T. Prosen, Exact dynamics in dual-unitary quantum circuits, Phys. Rev. B **101**, 094304 (2020).

[11] B. Gutkin, P. Braun, M. Akila, D. Waltner, and T. Guhr, Local correlations in dual-unitary kicked chains, Phys. Rev. B **102**, 174307 (2020).

[12] P. W. Claeys and A. Lamacraft, Maximum velocity quantum circuits, Phys. Rev. Research **2**, 033032 (2020).

[13] B. Bertini and L. Piroli, Scrambling in Random Unitary Circuits: Exact Results, Phys. Rev. B **102**, 064305 (2020).

[14] I. Reid and B. Bertini, Entanglement barriers in dual-unitary circuits, Phys. Rev. B **104**, 014301 (2021).

[15] R. Suzuki, K. Mitarai, and K. Fujii, Computational power of one- and two-dimensional dual-unitary quantum circuits, Quantum **6**, 631 (2022).

[16] S. A. Rather, S. Aravinda, and A. Lakshminarayan, Creating Ensembles of Dual Unitary and Maximally Entangling Quantum Evolutions, Phys. Rev. Lett. **125**, 070501 (2020).

[17] P. Facchi, G. Florio, G. Parisi, and S. Pascazio, Maximally multipartite entangled states, Phys. Rev. A **77**, 060304 (2008).

[18] D. Goyeneche and K. Życzkowski, Genuinely multipartite entangled states and orthogonal arrays, Phys. Rev. A **90**, 022316 (2014).

[19] P. Hosur, X.-L. Qi, D. A. Roberts, and B. Yoshida, Chaos in quantum channels, J. High Energy Phys. 02 (2016) 004.

[20] D. Goyeneche, D. Alsina, J. I. Latorre, A. Riera, and K. Życzkowski, Absolutely maximally entangled states, combinatorial designs, and multiunitary matrices, Phys. Rev. A **92**, 032316 (2015).

[21] M. Gaeta, A. Klimov, and J. Lawrence, Maximally entangled states of four nonbinary particles, Phys. Rev. A **91**, 012332 (2015).

[22] D. Goyeneche, Z. Raissi, S. Di Martino, and K. Życzkowski, Entanglement and quantum combinatorial designs, Phys. Rev. A **97**, 062326 (2018).

[23] F. Huber and N. Wyderka, Table of AME states. Online available, 2021, https://www.tp.nt.uni-siegen.de/+fhuber/ame.html.

[24] F. Huber, C. Eltschka, J. Siewert, and O. Gühne, Bounds on absolutely maximally entangled states from shadow inequalities, and the quantum MacWilliams identity, J. Phys. A: Math. Theor. **51**, 175301 (2018).

[25] S. A. Rather, A. Burchardt, W. Bruzda, G. Rajchel-Mieldzioć, A. Lakshminarayan, and K. Życzkowski, Thirty-Six Entangled Officers of Euler: Quantum Solution to a Classically Impossible Problem, Phys. Rev. Lett. **128**, 080507 (2022).

[26] F. Pastawski, B. Yoshida, D. Harlow, and J. Preskill, Holographic quantum error-correcting codes: toy models for the bulk/boundary correspondence, J. High Energy Phys. 06 (2015) 149.

[27] T. Kibe, P. Mandayam, and A. Mukhopadhyay, Holographic spacetime, black holes and quantum error correcting codes: A review, Eur. Phys. J. C **82**, 463 (2022).

[28] J. Berger and T. J. Osborne, Perfect tangles, arXiv:1804.03199 [quant-ph].

[29] R. J. Harris, N. A. McMahon, G. K. Brennen, and T. M. Stace, Calderbank-Shor-Steane holographic quantum error-correcting codes, Phys. Rev. A **98**, 052301 (2018).

[30] M. Doroudiani and V. Karimipour, Planar maximally entangled states, Phys. Rev. A **102**, 012427 (2020).

[31] C. Jonay, V. Khemani, and M. Ippoliti, Triunitary quantum circuits, Phys. Rev. Research **3**, 043046 (2021).

[32] A. Bhattacharyya, Z.-S. Gao, L.-Y. Hung, and S.-N. Liu, Exploring the tensor networks/AdS correspondence, J. High Energy Phys. 08 (2016) 086.

[33] V. F. R. Jones, Planar algebras, I, arXiv:math/9909027 [math.QA].

[34] V. Jones and V. S. Sunder, *Introduction to Subfactors*, London Mathematical Society Lecture Note Series (Cambridge University Press, Cambridge, 1997).

[35] D. J. Reutter and J. Vicary, Biunitary constructions in quantum information, Higher Structures **3**, 109 (2019).

[36] V. Kodiyalam, Sruthymurali, and V. S. Sunder, Planar algebras, quantum information theory and subfactors, arXiv:1912.07228.

[37] U. Krishnan and V. S. Sunder, On Biunitary Permutation Matrices and Some Subfactors of Index 9, Trans. Amer. Math. Soc. **348**, 4691 (1996).

[38] P. Kos, T. Prosen, and B. Bertini, Thermalization dynamics and spectral statistics of extended systems with thermalizing boundaries, Phys. Rev. B **104**, 214303 (2021).

[39] J. Deschamps, I. Nechita, and C. Pellegrini, On some classes of bipartite unitary operators, J. Phys. A: Math. Theor. **49**, 335301 (2016).

[40] J. Gütschow, S. Uphoff, R. F. Werner, and Z. Zimborás, Time asymptotics and entanglement generation of Clifford quantum cellular automata, J. Math. Phys. **51**, 015203 (2010).

[41] P. W. Claeys, J. Herzog-Arbeitman, and A. Lamacraft, Correlations and commuting transfer matrices in integrable unitary circuits, SciPost Physics **12**, 007(2022).

[42] P. Zanardi, Entanglement of quantum evolutions, Phys. Rev. A **63**, 040304(R) (2001).

[43] P. W. Claeys and A. Lamacraft, Ergodic and Nonergodic Dual-Unitary Quantum Circuits with Arbitrary Local Hilbert Space Dimension, Phys. Rev. Lett. **126**, 100603 (2021).

[44] T. Prosen, Many Body Quantum Chaos and Dual Unitarity Round-a-Face, Chaos **31**, 093101 (2021).

[45] L. Clarisse, S. Ghosh, S. Severini, and A. Sudbery, Entangling power of permutations, Phys. Rev. A **72**, 012314 (2005).

[46] A. S. Hedayat, N. J. Sloane, and J. Stufken, *Orthogonal Arrays: Theory and Applications* (Springer, New York, 1999).

[47] J. Egan and I. M. Wanless, Enumeration of MOLS of small order, Math. Comp. **85**, 799 (2016).

[48] R. K. Brayton, D. Coppersmith, and A. J. Hoffman, Self-orthogonal Latin squares of all orders $n \neq 2, 3, 6$, Bull. Amer. Math. Soc. **80**, 116 (1974).

[49] V. G. Drinfeld, "On some unsolved problems in quantum group theory, in *Quantum Groups*, edited by P. P. Kulish (Springer, Berlin, Heidelberg, 1992), pp. 1–8.

[50] P. Etingof, T. Schedler, and A. Soloviev, Set-theoretical solutions to the quantum Yang-Baxter equation, Duke Math. J. **100**, 169 (1999).

[51] W. Rump, Braces, radical rings, and the quantum Yang-Baxter equation, J. Alg. **307**, 153 (2007).

[52] T. Gombor and B. Pozsgay, Superintegrable cellular automata and dual unitary gates from Yang-Baxter maps, SciPost Phys. **12**, 102 (2022).

[53] Ö. Akgün, M. Mereb, and L. Vendramin, Enumeration of set-theoretic solutions to the Yang-Baxter equation, Math. Comp. **91**, 1469 (2022).

[54] A. Konovalov and L. Vendramin, YangBaxter (package for GAP)." Online available, 2021, https://github.com/gap-packages/YangBaxter.

[55] W. Helwig, Absolutely Maximally Entangled Qudit Graph States, arXiv:1306.2879 [quant-ph].

[56] L. Chen and D. L. Zhou, Graph states of prime-power dimension from generalized CNOT quantum circuit, Sci. Rep. **6**, 27135 (2016).

[57] W. Tadej and K. Zyczkowski, A concise guide to complex Hadamard matrices, Open Syst. Inf. Dyn. **13**, 133 (2006).

[58] S. Gopalakrishnan and B. Zakirov, Facilitated quantum cellular automata as simple models with non-thermal eigenstates and dynamics, Quantum Sci. Technol. **3**, 044004 (2018).

[59] S. Gopalakrishnan, Operator growth and eigenstate entanglement in an interacting integrable Floquet system, Phys. Rev. B **98**, 060302(R) (2018).

[60] F. J. Dyson and H. Falk, Period of a Discrete Cat Mapping, Am. Math. Month. **99**, 603 (1992).

[61] I. Wanless, Data on mutually orthogonal Latin squares (MOLS). Online available, https://users.monash.edu.au/~iwanless/data/MOLS/.

[62] R. Boll, Classification of 3d Consistent Quad-Equations, J. Nonlin. Math. Phys. **18**, 337 (2011).